Rapid Diffusion Monte Carlo Algorithms for Fluid Dynamic Permeability

Chi-Ok Hwang* Michael Mascagni† James A. Given‡

December 11, 2000

Abstract

In our previous study, [8], we described two efficient methods of estimating the fluid permeability of a porous medium as a function of the medium's porosity. These methods use the statistics of Brownian particles diffusing near a sample of the medium. The Brownian trajectories are constructed by using the Green's function first-passage method. These trajectories are built up as a series of discrete jumps, each jump leaving the center of a first-passage domain and landing at a point on its first-passage surface. Using transition probabilities that are sampled from the Laplacian Green's function for the geometry of the first-passage domain, each landing position is determined. This is an exact sampling method that is an acceleration of the walk on spheres method. The first of these two first-passage methods estimates permeability in terms of the fluid-dynamic penetration depth, identifying the latter with a penetration property of Brownian paths. The second method computes the effective electrostatic capacitance of the sample and relates it, via angle-averaging theorems, to the translational hydrodynamic friction, and then uses a mean-field approximation to equate the latter quantity to the permeability of the porous medium. For the sampling of porous media, we exploited our "sharp-boundary" sampling method. We improve on our previous permeability estimates using a refinement of the sharp-boundary sampling algorithm. In our new algorithm, we decrease the number of jumps required to simulate a complete Brownian path. This is accomplished by starting the paths directly on the spherical sharp boundary of the porous medium sample. This is mathematically equivalent to the old method, but both much faster and more numerically precise. In fact, our new method is about three times faster, and the new method provides better permeability estimates at low porosities. The new method produces trajectories with many fewer jumps on average. Since the computational cost of these methods is roughly proportional to number of jumps, this explains the speed up. Moreover, our improvements in precision and execution time are most dramatic when simulating low porosity sample. With our previous method, the low porosity case was the most demanding. In several of the cases studied here, our permeability results are identical to those obtained from detailed deterministic solution of the Stokes equations, to within statistical error. Finally, the reduction in the average number of jumps reduces the effective dimensionality of the problem. This opens the possibility of further acceleration though the use of quasirandom numbers, [2].

*Department of Computer Science, Florida State University, 203 Love Building, Tallahassee, FL 32306-4530, **USA**, E-mail: chwang@cs.fsu.edu

†Department of Computer Science, Florida State University, 203 Love Building, Tallahassee, FL 32306-4530, **USA**, E-mail: mascagni@cs.fsu.edu, URL: http://www.cs.fsu.edu/~mascagni

‡Angle Inc., 7406 Alban Station Court, Suite A112, Springfield, VA 22150 **USA**, E-mail: given@angleinc.com

1 Introduction

If we have a porous medium with a pressure difference, ΔP, across a characteristic distance of L, Darcy's law states that the volumetric flux, F, of a fluid through this porous medium is proportional to the pressure gradient. The constant of proportionality is the permeability, k:

$$F = k\frac{\Delta P}{L}. \tag{1}$$

Permeability has dimensions of area, and the permeability of a porous medium made up of a union of impermeable objects is a function of the medium's porosity. The porosity of a medium is the volume fraction of void space in the medium. High porosity results in high permeability while low porosity implies low permeability.

Many theoretical studies of porous media have attempted to estimate or bound fluid permeability, given the medium's average statistical properties, [19, 3, 13, 9, 1, 11], such as its porosity. Ideas employed have included the Λ parameter, [9], and the mean survival time (inverse reaction rate), [1, 14]. One can calculate the permeability of porous media by solving the Stokes equation for each statistical sample of the medium, using a deterministic method, and then averaging the results, [13]. This is computationally very expensive. Employing the lattice Boltzmann method to the hydrodynamics speeds up these calculations; however, the discretization error imposed causes inaccuracy in permeability, especially at low porosities, [3, 11].

One basic class of theoretical porous media models allows one to study either packed beds or consolidated porous media such as sandstone. These models consist of ensembles of equal-sized impermeable spherical inclusions immersed in a completely permeable medium. When used to model a packed bed, these spheres are non-overlapping; when used to model a consolidated porous medium, they are randomly located and freely overlapping.

The "**f**irst-**p**assage" (FP) method, [5], which we use to simulate Brownian motion in the continuum, is a refinement of the "**w**alk **o**n **s**pheres" (WOS) method for the efficient generation of Brownian trajectories, [15, 18, 12]. The FP method constructs Brownian trajectories by using FP probabilities obtained from various Green's functions of the Laplace equation. The Green's functions used permit the exact sampling of FP probabilities in complicated geometries involving the union of spheres and planes. The FP method is substantially more efficient than WOS for diffusing particles very close to absorbing boundaries, [8], and this makes it ideal for the study of low-porosity materials.

It was first conjectured that Brownian motion might be used to compute the fluid permeability in general microstructures, [14], and in our previous study, [7, 8], we explored two efficient algorithms of this type for estimating the permeability of several classes of porous media models. Both these algorithms involved simulating average properties of paths traced out by diffusing particles that initiate outside a spherical sample of the porous medium and are absorbed on contact with the porous sample. In particular, we explored the **u**nit **c**apacitance (UC) method and the **p**enetration **d**epth (PD) method.

The UC method uses Brownian paths to calculate an effective capacitance, C, for a porous sample, [6]. This is the capacitance of a perfect conductor having its geometry identical to that of the sample. This capacitance is related, via an angle-averaging relation, to the translational hydrodynamic friction of the sample when viewed as an object moving through a viscous fluid, [6]. This latter quantity is related to the permeability of the sample by an analytic result, [4].

The latter, PD, method associates the hydrostatic "penetration depth" of the sample with a specific average property of Brownian paths diffusing near its surface, namely, the average radial distance, beyond the sample radius, that the diffusing particles have penetrated into the sample

at the time of absorption. The method then uses the standard relation between penetration depth and permeability to estimate the latter, [17].

For providing a consistent method for sampling a porous medium of a given porosity, a new sampling method, called the "sharp-boundary" method, was proposed and used with these two methods, [7, 8].

In this paper, we improve the permeability estimation methods by dispensing with the need for the launching sphere, where the diffusing particle normally initiates. Instead, we place the diffusing particles directly on the sampling sphere. Removing the need for the launching sphere reduces the average length of first-passage jumps and so improves efficiency. This, in effect, reduces the effective dimension of the problem, making this method more amenable to convergence acceleration via the use of quasirandom numbers. Also, these changes improve the accuracy of the UC method at low porosities.

2 Overview of the PD and UC Methods

We now briefly explain the PD and UC methods that we employ to calculate permeabilities. More detail on these methods can be found in our previous work, [8], and the curious reader is encouraged to consult this paper.

In the UC method, the translational hydrodynamic friction, f, for a wide variety of bodies is related to the corresponding electrostatic capacitance, C via an angle-averaging theorem, [6]:

$$f = 6\pi\eta C. \tag{2}$$

Here η is the fluid viscosity, and the above states that the translational hydrodynamic friction felt by a body moving relative to a viscous fluid is proportional to the electrostatic capacitance of the body, when viewed as a perfect conductor.

Assuming that a given spherical porous sample is much larger than either the average distance between spherical inclusions or the correlation length associated with their statistics, the media can be modeled as a homogeneous porous sphere of radius R with the appropriate porosity. The translational frictional coefficient is obtained by solving the linear Stokes equation for such a porous sphere,[4, 17]. The result is:

$$f = 6\pi\eta R G_0(\sigma)\{1 + \frac{3}{2\sigma^2} G_0(\sigma)\}^{-1}, \tag{3}$$

where the function $G_0(\sigma)$ is given by:

$$G_0(\sigma) = 1 - \frac{1}{\sigma}\tanh\sigma. \tag{4}$$

Here σ is the dimensionless quantity defined by:

$$\sigma = \frac{R}{\sqrt{k}}, \tag{5}$$

where R is the porous sample radius and k is the permeability.

For each porosity, there is a range of sample radii which are much larger than the average distance between spherical inclusions, but for which the ratio C/R will be far enough from unity to permit us to interpolate of the corresponding σ value using Eq. 3.

Eliminating the translational frictional coefficient between Eqs. 2 and 3, one finds a relation between the capacitance and the permeability to be:

$$\frac{C}{R} = G_0(\sigma)\{1 + \frac{3}{2\sigma^2}G_0(\sigma)\}^{-1}. \quad (6)$$

Obtaining C/R, the unit capacitance, via simulation, allows us to use Eq. 6 to obtain σ, and thus obtain the desired permeability estimate from Eq. 5. In addition, each estimate for C/R is obtained by sampling over an ensemble of different porous media constructed to have the same porosity. Thus, in this way, we can rapidly compute an ensemble average with a Monte Carlo method that can deal with geometries of the different elements of the ensemble much more effectively than any deterministic method known.

C/R in the UC method varies rapidly as a function of R or σ. However, the composition of these two relations for computing k contains a broad plateau region, i.e., a large range of sample radii for which the predicted permeability is essentially constant, [8]. This property solves the problem of surface artifacts, so that we can accurately determine a bulk property, such as permeability.

The PD method is defined as follows. If we solve the Stokes equation for flow near a homogeneous planar porous interface it can be shown that $\sqrt{k}$ measures the"penetration depth", *i.e.* the distance that the flow effectively penetrates into the porous medium. We identify the penetration depth with the difference, ℓ, between the average radial position at which the diffusing particles are absorbed and the actual sample radius, thus yielding the approximate relation:

$$k = \ell^2. \quad (7)$$

We thus determine ℓ by direct simulation using the FP algorithm to produce the required Brownian paths. It is important to note that the same Brownian paths may be used to obtain permeability estimates via both the UC and PD methods. Thus, the same Brownian trajectory is used to obtain both estimates simultaneously.

The porous media sample, which is a union of impermeable inclusion spheres of radius a, is constructed as follows. We first place the centers of inclusion spheres into a large sphere of radius $(R+a)$ by random sequential addition, [16], for a given porosity, which places overlapping spherical inclusions sequentially and randomly until the desired porosity is reached. We then define the boundary of the actual sample by drawing a sphere of radius R, and allowing this sphere to freely intersect inclusions already placed. The sample is then defined to be all of the void phase, all inclusions, and all fragments of inclusions, that are contained in this sample sphere of radius R. With this sharp boundary, the porosity in the actual sample boundary is maintained uniformly up to the boundary. We call this new sampling method the "sharp-boundary" method.

3 Comparison of The New and Old Algorithms

In this section, we introduce a new and simpler FP algorithm for the calculation of permeability, and compare its efficiency with our old FP algorithm. With the previous FP method with "sharp-boundary" sampling, a Brownian particle initiates on a "launching sphere" which encloses the spherical porous media sample. We then use the WOS algorithm at the first stage to decide whether the diffusing particle is absorbed in the sampling sphere within a δ-thick layer around the sample, called the δ absorption layer, or whether the particle goes to infinity. However, since the porous medium itself is encased in a spherical sharp boundary, it is computationally more efficient to start our walks on the sample boundary. The reason is that we compute only the first-passage probability of each walk, and the cumulative first hitting location of walks with simulated starting locations at infinity. By starting our walks directly on the spherical sample boundary, we can drastically reduce the number of steps in the Brownian paths and remove the error associated with the δ-absorption layer. Even though the error associated with the absorption layer is small,

it becomes more important at lower porosities. The reason is that the unit capacitance at low porosities is very close to unity, and so often the value of the unit capacitance exceeds unity at extreme low porosities due to statistical fluctuation. The errors associated with the absorption points in the δ-absorption layer affect the PL estimate, even more so at low porosities. In addition, since the computational cost of each first-passage jump is roughly proportional to the number of steps in the walk, we also speed up the computation as well.

As an example of the computational improvement provided by our new method, we compare CPU times for porous media composed of overlapping spheres, and polydispersed overlapping spheres. The results given in Table 1 show that our new algorithm achieves a consistent speed up of about a factor of three over the old algorithm using identical convergence criteria. This table shows that we reduce the average number of first-passage jumps by at least a factor of five, and that we reduce the computational time at least by a factor of two. The reduction in the number of first-passage jumps is much greater than the overall CPU time because in the new method each step has a higher probability of striking the porous medium and therefore terminating. A first-passage jump that strikes the medium is more costly as we must use complicated boundary Green's functions to choose the hitting location, [8].

Another effect of starting our walks directly on the sample sphere is that now there is a nontrivial probability that the walk will terminate with its initial placement. Since we now choose a walker's starting location uniformly on the sample sphere, the probability of termination on the first step will be equal to the fraction of the sample sphere's area that intersects the media inclusions. This fraction clearly goes to one as porosity decreases. Thus, one would expect that as porosity decreases the average number of first-passage jumps would decrease, and hence the new method would not only be more accurate but also more efficient at low porosities. Figure 1 plots the average number of first-passage jumps as a function of porosity. This plot confirms our conjecture on the increasing behavior of this average with increasing porosity. It is somewhat paradoxical that our new algorithm gets more efficient for more difficult, low porosity, problems.

4 Computational Results

Finally, we present some computational results that confirm that our new method works at least as well as our old method in accurately computing permeabilities of the samples of porous media. The computational results for randomly overlapping monosized spherical inclusions are shown in Figures 2 and 4. Our estimates using the new method agree well with the Stokes solution for all porosities compared, [11]. It is noteworthy that we can use bigger sampling radius (R=50) at low porosities because we solved the problem that the unit capacitance exceeds unity at low porosities due to statistical fluctuation. We reduced the error due to the δ-absorption layer by removing the layer on the sampling sphere.

We next apply our new versions of the UC and PD methods with sharp-boundary sampling to permeability models of packed beds composed of polydispersed overlapping, randomly placed, impenetrable spherical inclusions. The inclusion sphere radii are chosen at random from the values 1.5, 3.5, 5.5, and 7.5. We compare our results with the available deterministic numerical solutions of the Stokes equation, [11]. Figures 3 and 5 show that our methods agree well with these non-Monte Carlo methods.

Our methods give very good results for all models of porous media tested. New estimates are better at low porosities in random media than the old method. The new method removes the error due to the absorption layer on sampling sphere when we eliminate the launching sphere. It is very unfortunate that so few high quality estimates exists even for the simple models studied here for us to use for our comparisons. We note; however, that these porosity models have been standards for

theoretical study for decades. Our methods predict permeabilities for a large class of homogeneous and isotropic porous media, in the medium and high porosity regimes from a porosity of 0.1 up to 0.9.

An important point to note about both the new and old FP methods is that they both are very fast compared with other methods. Our computations were written in `FORTRAN` to be run on parallel computers using MPI. Using 10 233MHz Pentium II processor nodes, with one porous sample per node, one million diffusing particles for each porous sample and porosity, and 10 porosities, it takes about 2 to 3 hours per set of calculations to generate one published figure's data. Using the boundary-element or finite-element methods to solve the Stokes equation in a sample of porous media can require the same amount of time to do this set of calculations for a single value of porosity. However, while our Monte Carlo method becomes more efficient with decreasing porosity, we believe that there is no such dependence in deterministic methods for this problem. In fairness, it should be noted that if one uses one of the deterministic methods one can obtain other physical quantities such as the local velocity and pressure field, yet if only permeability is required our Monte Carlo methods are much more efficient.

5 Conclusions and Future Work

We have shown improvements in our new FP algorithms for computing permeabilities in both speed and in permeability estimates at low porosities. These improvements make a very good method even better. In fact, in some of the cases studied here, our results are statistically equivalent to those obtained via the extremely time-consuming deterministic solution of the Stokes equations for the permeability. And, because of the reduction in first-passage jumps, the new method reduces the effective dimension of this problem. In the near future we plan to exploit this dimensional reduction by using quasirandom numbers to generate the diffusion trajectories. We hope that this, like other successful quasi-Monte Carlo methods, will accelerate the convergence of our method, thus providing yet another significant efficiency improvement.

In related work, we have been using these FP algorithms and their variations to compute both the effective conductivity and effective diffusivity of composite materials. In addition, we have been expanding the types of problems and the types of geometries which we can solve exactly by related methods by expanding the families of Green's functions that we use to build up our Brownian paths. We feel that these more powerful variants of the described methods will be powerful tools in solving problems in a wide variety of application areas.

Acknowledgements

We give special thanks to Nicos Martys, Eduardo Glandt and Dan Rothman for their useful information and comments. We thank Joe Hubbard and Jack Douglas for useful discussions. We are especially grateful to Nicos Martys for sharing with us the raw simulation data used in Figs. 2-5, [11].

References

[1] M. Avellaneda and S. Torquato, "Rigorous link between fluid permeability, electrical conductivity and relaxation times for transport in porous media," *Phys. Fluids A*, **3**: 2529 (1991).

[2] R. E. Caflisch, "Monte Carlo and Quasi-Monte Carlo Methods," Acta Numerica, **7**: 1–49 (1998).

[3] A. Cancelliere, C. Chang, E. Foti, D. H. Rothman and S. Succi, "The permeability of a random medium: Comparison of simulation with theory," *Phys. Fluids A*, **2(12)**: 2085 (1990).

[4] B. U. Felderhof, "Frictional properties of dilute polymer solutions; III. Translational-friction coefficient," *Physica A* **80**: 63 (1975).

[5] J. A. Given, J. B. Hubbard, and J. F. Douglas, "A first-passage algorithm for the hydrodynamic friction and diffusion-limited reaction rate of macromolecules," *J. Chem. Phys.*, **106(9)**: 3721 (1997).

[6] J. B. Hubbard and J. F. Douglas, "Hydrodynamic friction of arbitrarily shaped Brownian particles," *Phys. Rev. E*, **47**: 2983 (1993).

[7] C. O. Hwang, *A New Fluid Permeability Estimation in Periodic Grain Consolidation Models and Nonoverlapping and Overlapping Mono-sized Sphere Models of Porous Media*, Doctoral Dissertation, University of Southern Mississippi, (1999).

[8] C. O. Hwang, J. A. Given, and M. Mascagni, "On the rapid estimation of permeability for porous media using Brownian motion paths," *Phys. Fluids*, **12(7)**: 1699–1709 (2000).

[9] D. L. Johnson, J. Koplik, and L. M. Schwartz, "New pore-size parameter characterizing transport in porous media," *Phys. Rev. Lett.*, **57**: 2564 (1986).

[10] R. E. Larson and J. J. L. Higdon, "A periodic grain consolidation model of porous media," *Physics Fluids A*, **1**: 38 (1989).

[11] N. S. Martys, S. Torquato, and D. P. Bentz, "Universal scaling of fluid permeability for sphere packings," *Phys. Rev. E*, **50**: 403 (1994).

[12] K. K. Sabelfeld, *Monte Carlo Methods in Boundary Value Problems*, Springer-Verlag: Berlin, (1991).

[13] L. M. Schwartz, N. Martys, D. P. Bentz, E. J. Garboczi and S. Torquato, "Cross-property relations and permeability estimation in model porous media," *Phys. Rev. E*, **48**, 4584 (1993).

[14] S. Torquato, "Relationship between permeability and diffusion-controlled trapping constant of porous media," *Phys. Rev. Lett.*, **64**: 2644 (1990)

[15] S. Torquato and I. C. Kim, "Efficient simulation technique to compute effective properties of heterogeneous media," *Appl. Phys. Lett.*, **55(18)**: 1847 (1989).

[16] B. Widom, "Random Sequential Addition of Hard Spheres to a Volume," *J. Chem. Phys.*, **44(10)**: 3888 (1966).

[17] F. W. Wiegel, *Fluid Flow through Porous Macromolecular Systems*, Springer-Verlag: Berlin, Heidelberg, New York, (1980).

[18] L. H. Zheng and Y. C. Chiew, "Computer simulation of diffusion-controlled reactions in dispersions of spherical sink," *J. Chem. Phys.*, **90(1)**: 322, (1989).

[19] H.-X. Zhou, "Calculation of translational friction and intrinsic viscosity. I. General formulation for arbitrarily shaped particles," *Biophys. J.*, **69**: 2286 (1995).

Table 1: Running time and average # of FP jumps

	CPU time (secs)		average # of FP jumps	
	Old	New	Old	New
Overlapping	116.78	46.48	93	12
Polydispersed Overlapping	158.98	77.54	119	20

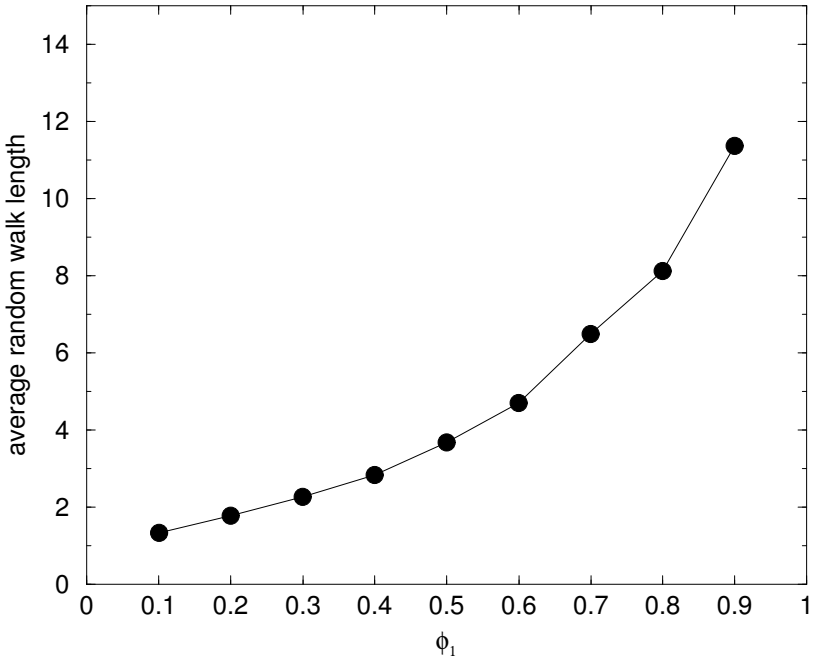

Figure 1: The average number of first-passage jumps versus porosity for randomly overlapping spheres of radius a = 1.0. As porosity decreases, the average number of first-passage jumps decreases.

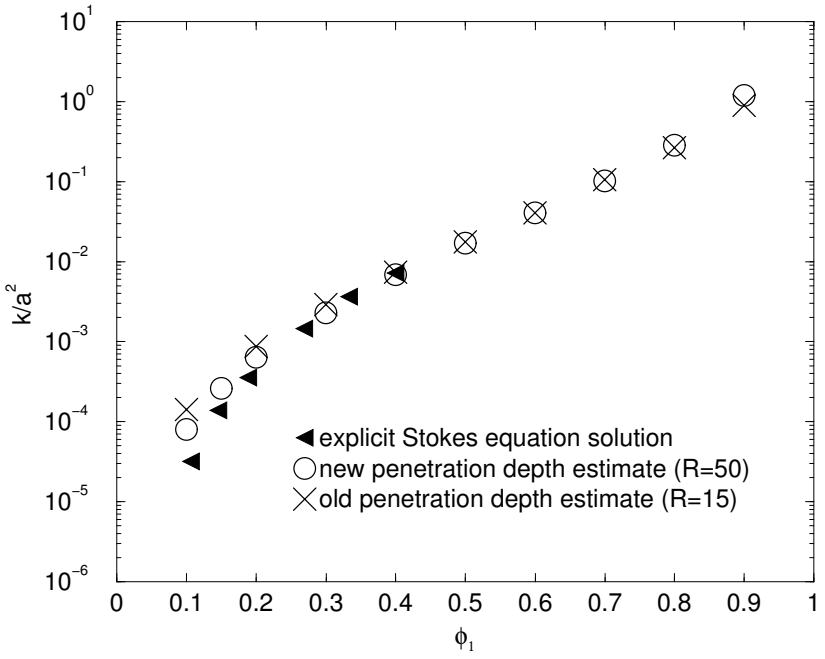

Figure 2: The dimensionless permeability k/a^2 versus porosity for randomly overlapping spheres of radius a = 1.0. The crosses are our old PD estimates with the sharp-boundary sampling method, the circles are our new PD estimates with the sharp-boundary sampling method, and the left triangles are the overlapping sphere bed data points from a finite-difference solution of the Stokes equation.

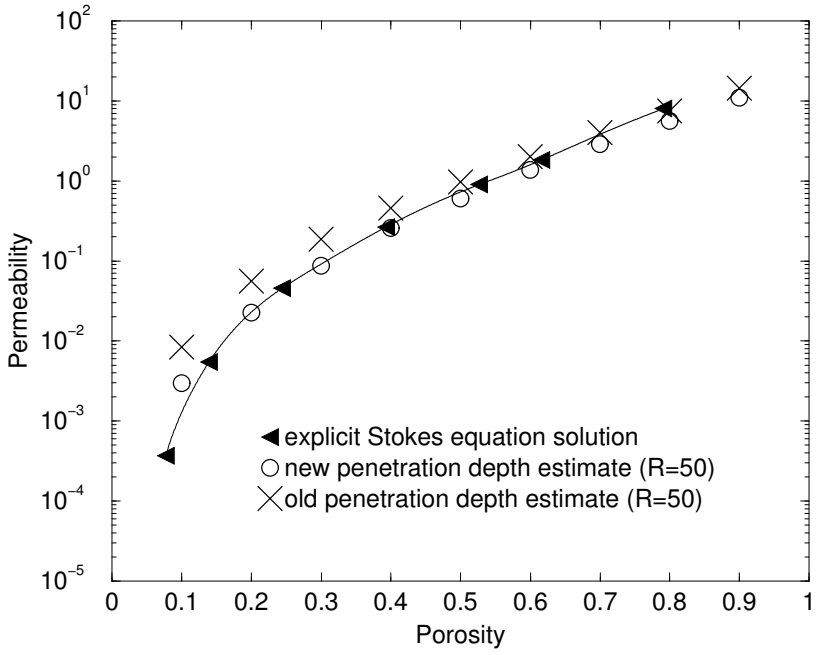

Figure 3: Permeability k versus porosity for a matrix constituted by a polydispersed mixture of randomly overlapping impermeable spheres with the sharp-boundary sampling method; the sphere radii are chosen to have the four values $a = \{1.5, 3.5, 5.5, 7.5\}$ with equal probability. Here the sample radius $R = 50.0$.

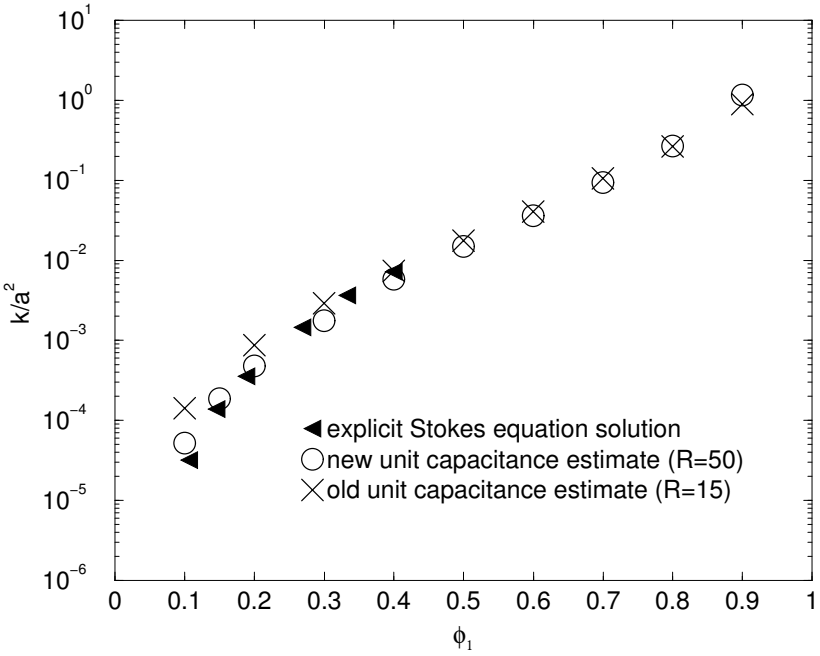

Figure 4: The dimensionless permeability k/a^2 versus porosity for randomly overlapping spheres of radius a = 1.0. The circles are our new UC estimates with the sharp-boundary sampling method, the crosses are our old UC estimates with the sharp-boundary sampling method, and the left triangles are the overlapping sphere bed data points from a finite-difference solution of the Stokes equation.

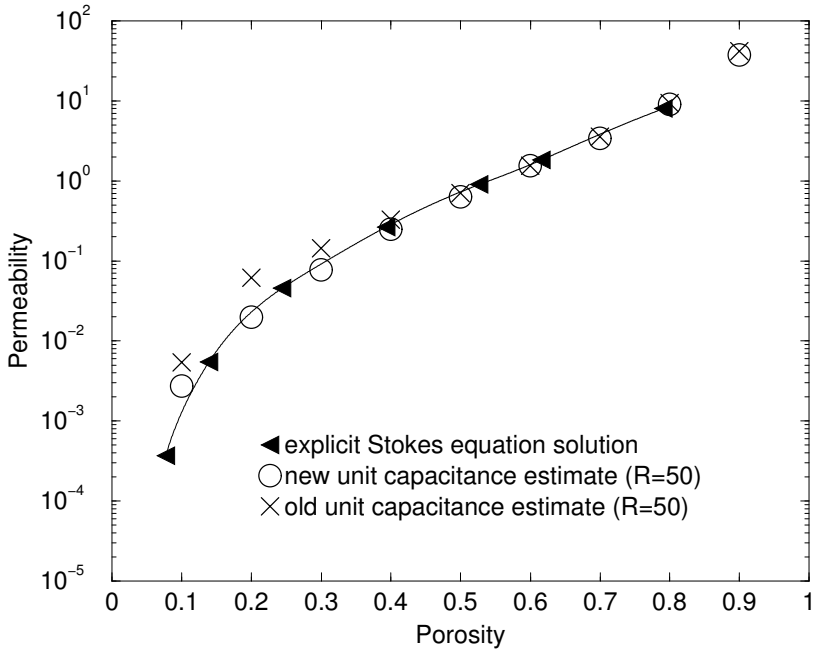

Figure 5: Permeability k versus porosity for a matrix constituted by a polydispersed mixture of randomly overlapping impermeable spheres with the sharp-boundary sampling method; the sphere radii are chosen to have the four values $a = \{1.5, 3.5, 5.5, 7.5\}$ with equal probability. Here the sample radius $R = 50.0$.